

A simple method for N - M interaction diagrams of circular reinforced concrete cross-sections

Raffaele Di Laora¹, Carmine Galasso², George Mylonakis³, and Edoardo Cosenza⁴

¹Assistant Professor, Dipartimento di Ingegneria, Università degli Studi della Campania “Luigi Vanvitelli”, Aversa (CE), Italy

²Associate Professor, Department of Civil, Environmental & Geomatic Engineering, University College London, London, UK

³Professor, Department of Civil Engineering, University of Bristol, Bristol, UK; Professor, University of Patras, Greece; Adjunct Professor, University of California, Los Angeles (CA), USA

⁴Professor, Dipartimento di Strutture per l’Ingegneria e l’Architettura, Università degli Studi di Napoli “Federico II”, Naples, Italy

Running head: N - M interaction diagrams of circular RC cross-sections

Corresponding author: Carmine Galasso, Department of Civil, Environmental & Geomatic Engineering, University College London, Gower St, WC1E 6BT, London, UK, c.galasso@ucl.ac.uk

ABSTRACT

A novel analytical expression is derived for the ultimate capacity interaction diagram (i.e., axial compression, N - bending moment resistance, M) of reinforced concrete (RC) columns with circular cross-section. To this aim, the longitudinal rebar arrangement is replaced with a thin steel ring equivalent to the total steel area; moreover, according to modern design

1 approaches, simplified stress-strain relationships for concrete and reinforcing steel are used.
2 Illustrative applications demonstrate that the ultimate capacity computed by the proposed
3 analytical approach agrees well with the results obtained by rigorous methods based on
4 consolidated numerical algorithms. The new solution allows for a rapid, accurate assessment
5 of circular cross-section capacity by means of hand calculations; this is especially useful at
6 the conceptual design stage of various structural and geotechnical systems. The solution can
7 be easily extended to more general configurations, such as multiple steel rings and composite
8 concrete-steel sections.

9

10 **Keywords:** reinforced concrete, circular cross-section, interaction diagram, simplified
11 formulation, analytical solution.

12

13 **INTRODUCTION**

14 Reinforced concrete (*RC*) structural members with circular cross-section are widely used in
15 structural and geotechnical engineering applications. Typical examples include columns in
16 moment-resisting frames, foundation piles and contiguous pile walls. The widespread use of
17 circular cross-sections in structural members is mainly due to their simplicity of construction
18 as well as to their identical stiffness and strength features in all horizontal directions.
19 However, while the design of rectangular *RC* cross sections may be easily performed (even
20 by hand calculations, under some simplifying assumptions), the analysis is more complex in
21 the case of circular cross-sections. In absence of analytical solutions, the assessment of axial
22 compression-bending moment resistance (*M-N*) interaction domains is performed numerically.
23 Research on the topic includes integration methods for both rectangular and circular *RC*
24 cross-sections based on analytical and numerical algorithms (e.g., Bonet et al., 2006; Elevard,
25 1997; Brondum Nielsen, 1988; Davalath et al., 1988). For instance, Bonet et al. (2006)

1 presented a comparative study of different integration methods (both analytical and
2 numerical) of stresses in circular and rectangular RC cross-sections subjected to axial loads
3 and biaxial bending. The constitutive equation used for concrete is a parabola-rectangle from
4 Eurocode 2 (CEN, 2004). The comparison is performed in terms of accuracy and
5 computational speed of each investigated method. Similarly, Davalath et al. (1988) developed
6 a numerical procedure along with a computer code for the analysis of RC circular cross-
7 sections subjected to axial loads (compression or tension) and bending moments. Barros et al.
8 (2004) derived a closed-form solution for the optimal design of *RC* cross-sections, but only
9 for the rectangular shape. This method is valid for ultimate axial and (uniaxial) bending
10 loading; it relies on the use of a parabola-rectangle diagram for the concrete in compression.
11 Furthermore, Tumo et al. (2009) have presented an analytical approach for quantifying the
12 contribution of transverse reinforcement to the shear resistance of *RC* structural members of
13 solid and hollow circular cross-section. Recently, Trentadue et al. (2016) proposed closed-
14 form approximations of the *M-N* interaction domains for *RC* columns and concrete-filled
15 steel tubes with circular cross-section. A single analytical expression is provided for both
16 cases; however, one parameter (which is function of the mechanical ratio of the reinforcing
17 steel) of the proposed approach has still to be calibrated by means of a numerical
18 optimization procedure.

19 This note introduces a fully analytical, code-compatible procedure for the ultimate analysis of
20 *RC* circular cross-sections subjected to axial compression and bending. The study constitutes
21 an improvement over the method proposed in Cosenza et al. (2011). As in the previous study,
22 the equations are developed by assuming the reinforcement steel area as lumped into an
23 equivalent steel ring completely yielded, whereas the stress-block diagram is assumed for
24 concrete. In addition, design yield stress of steel is properly modified to obtain more accurate

1 results. Moreover, an analytical approximation is introduced to derive an analytical solution
2 for the computation of $M-N$ domains without iterations and/or numerical computation.

3 The rest of this paper is organized as follows. A review of code-based assumptions and
4 procedures for the assessment of the ultimate flexural capacity of RC cross-section is
5 presented first. The proposed analytical method is then described, introducing a simplified
6 approach for the derivation of $M-N$ domains. This is followed by a validation exercise for the
7 proposed method through a series of illustrative examples.

8

9 **CODE-BASED ASSESSMENT OF ULTIMATE FLEXURAL CAPACITY FOR RC** 10 **CROSS-SECTIONS**

11 Eurocode 2 (or EC2; CEN, 2004, *Sec. 6.1*) provides principles and rules for the assessment of
12 the ultimate flexural capacity of RC members, with or without axial force. To this end, the
13 following simplifying assumptions are made:

- 14 1. Plane cross-sections remain plane upon deformation, up to failure;
- 15 2. Strain in bonded reinforcement (whether in tension or in compression), is identical to that
16 in the surrounding concrete (i.e., perfect bonding exists between steel and concrete);
- 17 3. The tensile strength of the concrete is neglected;
- 18 4. Compressive stresses in concrete are derived according to pertinent idealized design
19 stress/strain relationships (*EC2, Sec. 3.1.7*);
- 20 5. Stresses in reinforcing bars are derived from corresponding design curves (*EC2, Sec.*
21 *3.2.7*);
- 22 6. Design strengths for concrete and steel are defined as $f_{cd} = \alpha_{cc} f_{ck} / \gamma_c$, $f_{yd} = f_{yk} / \gamma_s$,
23 respectively (*EC2, Secs. 3.1.6, 3.2.7*), where α_{cc} is a coefficient taking into account of long
24 term effects on compressive strength and of unfavorable effect resulting from the way the

1 load is applied¹, f_{ck} is the specified (i.e., characteristic, 5%) compressive strength of
2 concrete (cylinder strength) and f_{yk} is the specified yield stress of steel, γ_c and γ_s are
3 material safety factor according to Eurocode-like Load and Resistance Factor Design
4 (*LRDF*);

5 7. Material safety factors are $\gamma_c = 1.5$ for concrete and $\gamma_s = 1.15$ for steel (*EC2, Sec. 2.4.2.4*).

6 It is worth noting that all the above assumptions also hold in the case of *ACI 318-14 (2014)*.

7 The main difference is that the Eurocode-based approach to LFRD consists of reducing the
8 material ultimate strength values using their conservative percentiles (i.e., characteristic
9 values divided by material safety factors) as design values rather than applying safety factors
10 directly to the sectional strength (as in the *ACI 318-14* - see Iervolino and Galasso (2012) for
11 an extensive discussion on the topic). On the other hand, the specified compressive strength
12 of concrete and the specified yield strength for non-prestressed reinforcement in *ACI 318-14*
13 are directly used to compute the nominal flexural strength of a cross-section and this is
14 further reduced by a strength reduction factor in *ACI 318-14 (Chapter 21)*, ranging from 0.65
15 to 0.9 for moment, axial force, or combined moment and axial force.

16 According to points 4) and 5), a rigorous assessment of the ultimate flexural capacity may be
17 performed assuming a parabolic-rectangular relationship between the stress and
18 corresponding strain in the concrete in compression, whereas the steel may be idealized as an
19 elastoplastic-material (Fig. 1a). Such an analysis requires the use of integration procedures
20 and is thereby performed via computer codes—such as Biaxial software (Di Ludovico et al.,
21 2010). As a simpler alternative for the analysis and design of circular cross-sections at the
22 Ultimate Limit State (*ULS*), simplified stress-strain relationships may be utilized. For
23 instance, similarly to *ACI 318-14*, the stress distribution in the concrete may be assumed as a

¹ According to *EC2*, the value of α_{cc} for use in a Country should lie between 0.8 and 1 and the recommended values is 1.

1 rectangular stress block extended up to a depth, y , smaller than of the actual neutral axis
2 depth, x , and a magnitude, $f'_{cd} = f_{cd}$ equal to some fraction of the concrete compressive design
3 strength (generally, $y = 0.8x$ and $f'_{cd} = f_{cd}$ are assumed). This procedure means, in terms of
4 constitutive models of the materials, that concrete behaves as a perfectly plastic material after
5 reaching a specific threshold value of compressive strain whereas, below such a strain value,
6 it offers no resistance (Fig. 1b). In the framework of simplified methods, an elastic-plastic
7 stress-strain diagram for reinforcing steel, with a horizontal top branch without a strain limit,
8 is recommended. This latter assumption is well justified by experimental results (see for
9 example Galasso et al. 2014). Based on this assumption, the failure of the section always
10 occurs due to concrete crushing, i.e., when the maximum concrete strain is equal to an
11 ultimate strain value ϵ_{cu} (maximum concrete compressive strain) or to a second value ϵ_{c2}
12 when the section is all under compression. These deformation characteristics for concrete
13 depend on material strength; see for example Table 3.1 in *EC2*.
14 Due to these simplified assumptions, the computation of the flexural capacity is quite
15 straightforward by solving the equilibrium equations; yet, some iterations are necessary to
16 calculate the position of the neutral axis. A step-by-step presentation of the procedure is
17 provided in Cosenza et al., (2011).

18

19 **PROPOSED METHOD**

20 A rigorous analysis of circular cross-sections should be performed considering the actual
21 location of the reinforcement longitudinal bars. Such a condition does not allow a simple
22 analytical expression to be derived for the ultimate bending moment capacity. An
23 approximate formulation is possible by means of some straightforward idealizations;
24 specifically (Fig. 1c):

- 1 1. The actual longitudinal rebar arrangement is replaced by a thin steel ring with
2 equivalent total area A_s ;
- 3 2. The actual distribution of concrete stress is replaced by a rectangular diagram with an
4 “effective strength” $f'_{cd} = 0.9 f_{cd}$. This assumption concerns a specific EC2 provision
5 for circular cross-section: *if the width of the compression zone decreases in the*
6 *direction of the extreme compression fiber the value of the effective strength should be*
7 *reduced by 10%.*
- 8 3. The steel is considered to be at a yielding state, both in compression and tension,
9 contributing an “effective stress” $f'_{yd} = 0.95 f_{yd}$. The factor 0.95 has been calibrated
10 by the authors to minimize the discrepancies between the results from the proposed
11 approach and those obtained through more rigorous approaches, as discussed later in
12 in the paper’.

13 It is worth noting that these assumptions are equivalent to assuming a perfectly plastic
14 behavior for both steel and concrete, where the threshold strain value (a) separating
15 compression and tension for steel and (b) below which concrete offers no strength has a given,
16 positive value. Hence, for the assessment of the ultimate flexural capacity, regardless of the
17 actual strain profile, materials may be assumed to behave as rigid-plastic, and the resulting
18 (fictitious) neutral axis depth will coincide with the extension of the compressive zone.

19 Owing to these hypotheses, the condition of equilibrium between all the internal and external
20 forces applied to the cross-section may be written as:

$$21 \frac{R^2}{2} (2\theta - \sin 2\theta) f'_{cd} + \left(\frac{\theta}{\pi} \right) A_s f'_{yd} - \left(\frac{\pi - \theta}{\pi} \right) A_s f'_{yd} = N_{Ed} \quad (1)$$

22 where N_{Ed} is the applied axial force and θ is the angle defining the extension of compression
23 zone (Fig. 2), ideally varying from 0 (no compression) to π (the section is entirely

1 compressed). In Eq. (1), $(\theta/\pi) A_s$ and $(1-\theta/\pi) A_s$ are the cross-sectional areas of longitudinal
 2 reinforcement in compression and tension, respectively.

3 Multiplying each term in Eq. (1) by $\frac{2}{R^2 f'_{cd}}$, Eq. (1) may be reformulated as:

$$4 \quad (2\theta - \sin 2\theta) + 2\omega'\theta - 2\omega'(\pi - \theta) = 2\pi\nu' \quad (2)$$

5 where $\omega' = \frac{A_s f'_{yd}}{\pi R^2 f'_{cd}}$ and $\nu' = \frac{N_{Ed}}{\pi R^2 f'_{cd}}$ are the mechanical steel ratio and the design axial
 6 force normalized to the total cross-sectional concrete area of the member (the prime symbol
 7 “ ’ ” indicates that quantities are normalized by effective values of design strength – see point
 8 2 and 3 above).

9 Due to the transcendental nature of Eq. (2), the exact value of the angle θ may be found only
 10 iteratively (e.g., using the Newton's method). Nevertheless, an approximate explicit solution
 11 for θ is possible by substituting the term $\sin 2\theta$ in Eq. (2) with the parabola $16\theta(\pi/2 - \theta) / \pi^2$
 12 (for $\theta \leq \pi/2$). Consequently, Eq. (2) reduces to the second-order algebraic equation:

$$13 \quad \frac{16}{\pi^2} \theta^2 + 2 \left(1 + 2\omega' - \frac{4}{\pi} \right) \theta - 2\pi(\omega' + \nu') = 0 \quad (3)$$

14 which admits the positive solution:

$$15 \quad \theta = \left(\frac{\pi}{4} \right)^2 \left[- \left(1 + 2\omega' - \frac{4}{\pi} \right) + \sqrt{\left(1 + 2\omega' - \frac{4}{\pi} \right)^2 + \frac{32}{\pi} (\omega' + \nu')} \right] \quad (4)$$

16 A comparison between the exact values of θ obtained from Eq. (2) (exact relationship among
 17 θ , ν' and ω' may be found by fixing the values of θ and ν' , and calculating ω' , or fixing θ and
 18 ω' and calculating ν') and the correspondent estimates by means of Eq. (4) is offered in Fig. 3,
 19 as a function of dimensionless axial force ν' and reinforcement ratio ω' . Clearly, approximate
 20 estimates and exact values are almost coincident. Note that the simplified expression for θ is
 21 valid for $\nu' \leq 0.5$, i.e., $\theta < \pi/2$. Nevertheless, as the function $\theta(\nu')$ presents a symmetry point

1 around $(0.5, \pi/2)$, for $\nu' > 0.5$ the value of θ may be easily derived by symmetry
2 considerations.

3 Once evaluated θ , the design flexural capacity M_{Rd} is equal to the sum of the design flexural
4 resistance due to concrete, $M_{Rd,c}$, and the design flexural resistance due to steel, $M_{Rd,s}$. By
5 employing the quantities in Fig. 2, it is straightforward to show that ²:

$$6 \quad M_{Rd} = M_{Rd,c} + M_{Rd,s} = \frac{2}{3} R^3 \sin^3 \theta f'_{cd} + \frac{2}{\pi} (R-c) A_s \sin \theta f'_{yd} \quad (5)$$

7 where c is the concrete cover of cross-section; multiplying each term by $\frac{1}{2\pi R^3 f'_{cd}}$, Eq. (5)

8 may be rewritten as:

$$9 \quad \mu_{Rd} = \frac{1}{3} \frac{1}{\pi} \sin^3 \theta + \frac{\omega'}{\pi} \left(1 - \frac{c}{R}\right) \sin \theta \quad (6)$$

10 where $\mu_{Rd} = \frac{M_{Rd}}{2\pi R^3 f'_{cd}}$ is the dimensionless bending capacity of the cross-section. In this way,

11 the ultimate flexural capacity is expressed in general form as a function of the relevant
12 dimensionless parameters ω , ν and c/R .

13

14 **M-N INTERACTION DOMAINS**

15 The proposed method also allows for a simple computation of the interaction domains in an
16 analytical way, by simply varying the axial force and, thereby, retrieving the value of the
17 corresponding ultimate moment capacity by means of Eq. (5) or (6). In addition, the
18 simplified assumptions adopted here offer insight in the section layout at failure for some
19 peculiar situations corresponding to specific points on the domain. A sketch of a typical *M-N*

² Note that due to a clerical error, in the original work by Cosenza et al. (2011) the equation is reported with a wrong coefficient of 4/3 instead of 2/3.

1 (or, in dimensionless form, $\mu' - \nu'$) domain is reported in Fig. 4. Five (5) key points can be
2 identified.

3 - *Point A*. This corresponds to the extreme traction load the section can carry. In this
4 situation, no bending is allowed and the whole tensile force is carried by the steel, due
5 to the inherent assumption of no tensile strength offered by the concrete. The axial load
6 is thereby equal to the area of the steel A_s multiplied by its design strength f'_{yd} . In
7 dimensionless terms, it is immediate to derive that $\nu' = -\omega'$.

8 - *Point B*. This is the point symmetric to point A and corresponds to pure compression.
9 Both concrete and steel mobilize their strength in any point of the section. The
10 corresponding axial force is given by the sum of the steel capacity $f'_{yd}A_s$ and the
11 concrete capacity $f'_{cd} \pi R^2$. In dimensionless terms, $\nu' = 1 + \omega'$.

12 - *Point C*. This point is representative of pure bending. In such conditions, total
13 compression force associated to both concrete and steel must equal the tensile steel
14 force. This means that the depth of compression zone y_c is less than R . It is
15 straightforward to derive that y_c is an increasing function of the amount of
16 reinforcement ω and tends to R when reinforcement increases up to infinity, as in the
17 latter case concrete would give a negligible contribution compared to steel. A
18 simplified expression for the moment capacity under pure bending is presented in
19 Cosenza et al. (2011).

20 - *Point E*. This point corresponds to a failure condition with the same ultimate moment as
21 in *Point C* and an associated compressive force. This means that the increase in axial
22 force due to concrete and steel must not produce any bending moment and, therefore,
23 the depth of compression zone is equal to $(2R - y_c)$. The same result may be obtained
24 by considering that *Point E* is the one symmetrical to *Point C*. The axial force is equal

1 to the ultimate compressive load of an un-reinforced section ($\nu' = 1$). The presence of
2 the steel is, therefore, responsible for the finite moment capacity under normal load.

3 - *Point D*. This point is associated with the maximum bending capacity of the section,
4 occurring under a dimensionless axial force $\nu' = 0.5$. It is evident that the stress-block
5 diagram is extended up to a half cross-section, since any increase or decrease of the
6 compression zone would lead to a decrease in the bending moment capacity.

7 8 **VALIDATION OF THE PROPOSED METHOD**

9 Fig. 5 reports a comparison between the results obtained through the proposed approach and
10 a rigorous solution in the realm of the aforementioned assumptions 1-7. EC2 is used as the
11 reference code in this illustrative application; however, similar findings can be obtained by
12 using the *ACI 318-14* design framework. Results, expressed through dimensionless pairs ν
13 $': \mu'$, refer to a circular cross-section having a diameter of 50 cm and a concrete cover of 5
14 cm. Reinforcement is represented by 10, 20, 30 and 40 bars with a diameter $\phi = 16$ mm,
15 corresponding to reinforcement ratios ρ approximately equal to 1, 2, 3 and 4% (consistent
16 with detailing rules for local ductility of *RC* columns in seismic areas). Concrete and steel
17 have design strengths $f_{cd} = 14.2$ MPa ($\epsilon_{cu} = 0.35\%$) and $f_{yd} = 391$ MPa, respectively
18 (corresponding to $f_{ck} = 25$ MPa and $f_{yk} = 450$ MPa, the latter being the recommended value in
19 Italy). It is noted, by inspecting Figure 5, that the proposed method matches very closely the
20 rigorous results obtained by means of freeware Biaxial (available from the website of the
21 Italian Network of Earthquake Engineering University Labs, or ReLUIIS:
22 http://www.reluis.it/index_eng.html). The discrepancies from the rigorous analysis are of the
23 order of 1% for ν' values relevant to earthquake engineering applications (e.g., $\nu < 0.55$, ν'
24 < 0.61), whereas the method underestimates by 5% to 10% the extreme values corresponding
25 to a purely axial force. This is due to the simplifying assumption of reducing design strengths

1 employed in the proposed method. Numerical values, corresponding to ν' ratios ranging from
2 0 to 0.5, are also reported in Table 1 together with other formulations. In the table, M_{rd1} is the
3 most rigorous ultimate flexural capacity value of the cross-section computed by the Biaxial
4 software; M_{rd2} represents the same value but computed using the simplified stress-block
5 diagram for concrete under compression and assuming the effective strength of concrete
6 reduced by 10% according to *EC2*. (To this aim, an *ad hoc* MATHWORKS-MATLAB®
7 script was developed by the authors). Finally, M_{rd3} is evaluated according to Cosenza et al.
8 (2011), whereas M_{rd4} is the ultimate flexural capacity value of cross-section computed using
9 the proposed method. The mean absolute error of the proposed approach is 1.43%, on the
10 conservative side, offering better performance in predicting the flexural capacity over that
11 provided by both the stress-block analysis (2.61%) and the Cosenza et al. (2011) method
12 (3.54%). Note that the error provided by the proposed method is lower than the one by the
13 Trentadue et al. (2016) approach, which report an average discrepancy of 3.2% versus
14 numerical solutions. Further validation of the proposed approach could also be performed by
15 using results from experimental tests available in the literature. However, this is outside the
16 scope of this note. In fact, it can be quite challenging to gather reliable (especially in terms of
17 sample size, to allow statistically meaningful comparisons) and open (providing the required
18 input data to implement the proposed numerical solution) datasets of experimental tests for
19 RC members with circular cross-sections.

20

21 **CONCLUSIONS**

22 The choice of a circular cross-section for structural members is popular in both geotechnical
23 and structural design, due to simplicity of construction and equal strength under horizontal
24 loading in all directions. In comparison with rectangular cross-sections, no analytical
25 solutions are available to evaluate flexural capacity under a specified axial load. This paper

1 aimed at providing a simple, approximate analytical solution in the $M-N$ space which could
2 facilitate routine calculations. Comparison with rigorous numerical analyses indicates an
3 excellent performance of the proposed approach (maximum discrepancies of less than 5%,
4 typically less than 1%), outperforms existing simplified formulations, the latter being more
5 complicated and involving iterative, or even numerical procedures.

6

7 **REFERENCES**

- 8 American Concrete Institute (ACI) Committee 318, ACI 318-2014: *Building Code*
9 *Requirements for Structural Concrete and Commentary* 2014.
- 10 Barros H, Figueiras J. Reinforced concrete-design tables and abacus for the design of
11 sections: moment and axial load with *EC2*. In: FEUP edições. 2010.
- 12 Barros MHFM, Barros AFM, Ferreira CA. Closed form solution of optimal design of
13 rectangular reinforced concrete sections. *Engineering Computations* 2004; 21(7):761-776.
- 14 Bonet JL, Barros MHFM, Romero ML. Comparative study of analytical and numerical
15 algorithms for designing reinforced concrete section under biaxial bending. *Computers &*
16 *Structures* 2006; 8:31-32.
- 17 Brøndum Nielsen T. Ultimate Flexure Capacity of Circular and Annular Cracked Concrete
18 Sections. *ACI Structural Journal* 1988; 85(4):437-441.
- 19 CEN, European Committee for Standardisation. *Eurocode 2: Design of concrete structures.*
20 *Part 1-1: General rules and rules for buildings*; 2004
- 21 Cosenza E, Galasso C, Maddaloni G. A simplified method for flexural capacity assessment of
22 circular RC cross sections. *Engineering Structures* 2011; 33(3):942–946.
- 23 CS.LL.PP. DM 14 Gennaio, Norme tecniche per le costruzioni. *Gazzetta Ufficiale della*
24 *Repubblica Italiana* 29; 2008 (in Italian).

- 1 Davalath GSR, Madugula MKS. Analysis/Design of Reinforced Concrete Circular Cross-
2 Sections. *ACI Structural Journal* 1988; 85(6):617-623.
- 3 Di Ludovico M, Lignola GP, Prota A, Cosenza E. Nonlinear Analysis of Cross-Sections
4 under Axial Load and Biaxial Bending. *ACI Structural Journal* 2010; 107(4):390-399.
- 5 Elevard NJ. Axial Load-Moment Interaction for Cross-Sections Having Longitudinal
6 Reinforcement Arranged in a Circle. *ACI Structural Journal* 1997; 94(6):695-699.
- 7 Galasso C, Maddaloni G, Cosenza E. Uncertainty analysis of flexural overstrength for new
8 designed RC beams, *ASCE Journal of Structural Engineering* 2014; 140(7).
- 9 Iervolino I, Galasso C. Comparative assessment of load-resistance factor design for FRP-
10 reinforced cross sections, *Construction and Building Materials* 2012; 34:151-161.
- 11 Trentadue F, Quaranta G, Marano GC. Closed-form approximations of interaction diagrams
12 for assessment and design of reinforced concrete columns and concrete-filled steel tubes
13 with circular cross-section. *Engineering Structures* 2016; 127:594–601.
- 14 Turmo J, Ramos G, Aparicio AC. Shear Truss Analogy for Concrete Members of Solid and
15 Hollow Circular Cross-Section. *Engineering Structures* 2009; 31(2):455-465.

16
17
18
19
20
21
22
23
24
25

1 **List of Figure Captions**

2 Fig. 1 Assumptions on the constitutive behavior of materials and mobilized strength in the
3 different analysis methods.

4
5 Fig. 2 Stress distribution and formulae for the proposed method.

6
7 Fig. 3. Comparison between exact and approximate values of θ , as function of dimensionless
8 axial force ν' (left) and mechanical reinforcement ratio ω' (right).

9
10 Fig. 4. $N - M$ and $\nu' - \mu'$ domain through the proposed method.

11
12 Fig. 5. Comparison between results from proposed method and rigorous analysis.

13

14

15

16

17

18

19

20

21

22

23

24

25

26

27

28

29

30

31

32

33

34

35

36

1 **Table1. Comparison of results obtained by the proposed formula (M_{Rd4}) and other**
 2 **formulations from the literature, including the most rigorous numerical solution using**
 3 ***Biaxial* (M_{Rd1}).**

ν	ρ	M_{Rd1}	M_{Rd2}	M_{Rd3}	M_{Rd4}	$\frac{M_{Rd2} - M_{Rd1}}{M_{Rd1}}$	$\frac{M_{Rd3} - M_{Rd1}}{M_{Rd1}}$	$\frac{M_{Rd4} - M_{Rd1}}{M_{Rd1}}$
[-]	[%]	[kNm]	[kNm]	[kNm]	[kNm]	[%]	[%]	[%]
0	1	143.7	141.4	143.6	137.1	-1.60	-0.07	-4.59
	2	258.4	256.2	264.8	253.1	-0.85	2.48	-2.05
	3	365.7	361.2	377.9	361.2	-1.23	3.34	-1.23
	4	467.5	462.2	486.8	465.1	-1.13	4.13	-0.51
0.1	1	175.9	170.4	176.9	174.3	-3.13	0.57	-0.91
	2	283.6	277.3	290.2	281.6	-2.22	2.33	-0.71
	3	385.4	378.7	398.4	384.3	-1.74	3.37	-0.29
	4	483.9	475.7	504.0	484.6	-1.69	4.15	0.14
0.2	1	204.3	196.4	202.4	201.8	-3.87	-0.93	-1.22
	2	303.4	294.2	309.5	302.6	-3.03	2.01	-0.26
	3	399.2	390.0	414.0	401.4	-2.30	3.71	0.55
	4	494.6	484.7	517.1	499.0	-2.00	4.55	0.89
0.3	1	220.7	209.5	220.0	220.3	-5.07	-0.32	-0.18
	2	315.3	304.3	323.0	317.0	-3.49	2.44	0.54
	3	407.6	396.7	424.9	413.2	-2.67	4.24	1.37
	4	500.5	489.6	526.3	509.0	-2.18	5.15	1.70
0.4	1	228.0	217.8	229.9	227.3	-4.47	0.83	-0.31
	2	317.9	307.4	330.7	322.5	-3.30	4.03	1.45
	3	409.3	398.6	431.3	417.8	-2.61	5.38	2.08
	4	500.5	489.7	531.8	512.9	-2.16	6.25	2.48
0.5	1	224.7	215.2	233.0	227.3	-4.23	3.69	1.16
	2	314.4	304.6	333.2	322.6	-3.12	5.98	2.61
	3	404.4	394.5	433.3	417.8	-2.45	7.15	3.31
	4	494.6	484.6	533.5	512.9	-2.02	7.86	3.70

4
5
6
7
8
9
10
11
12
13
14
15
16
17
18
19
20
21
22
23

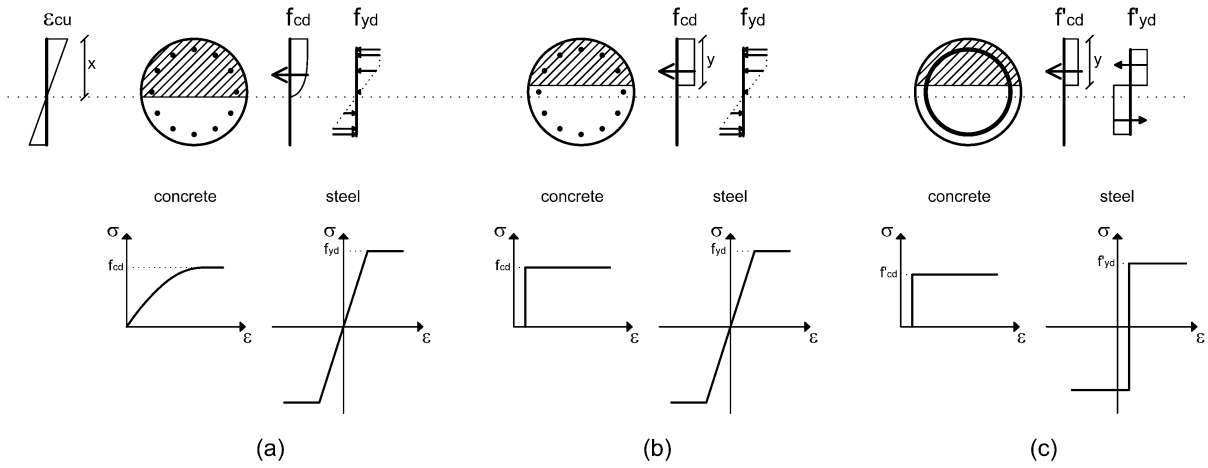


Figure 1

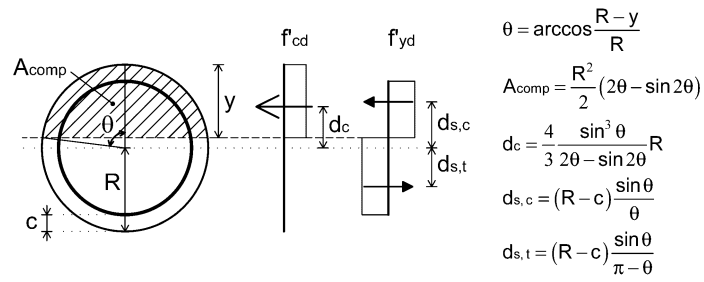


Figure 2

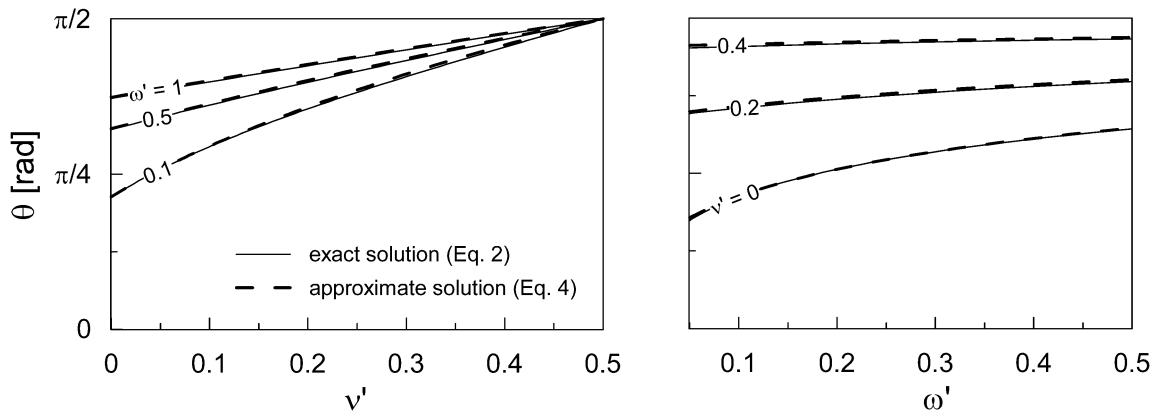


Figure 3

1
2
3

4
5
6

7
8
9

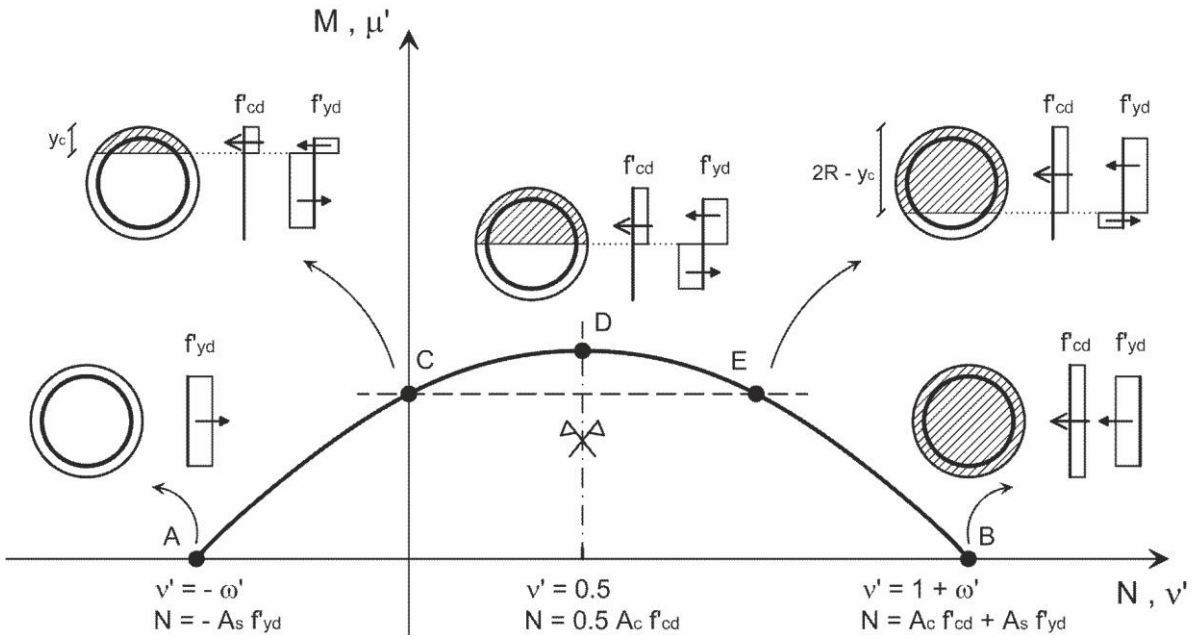


Figure 4

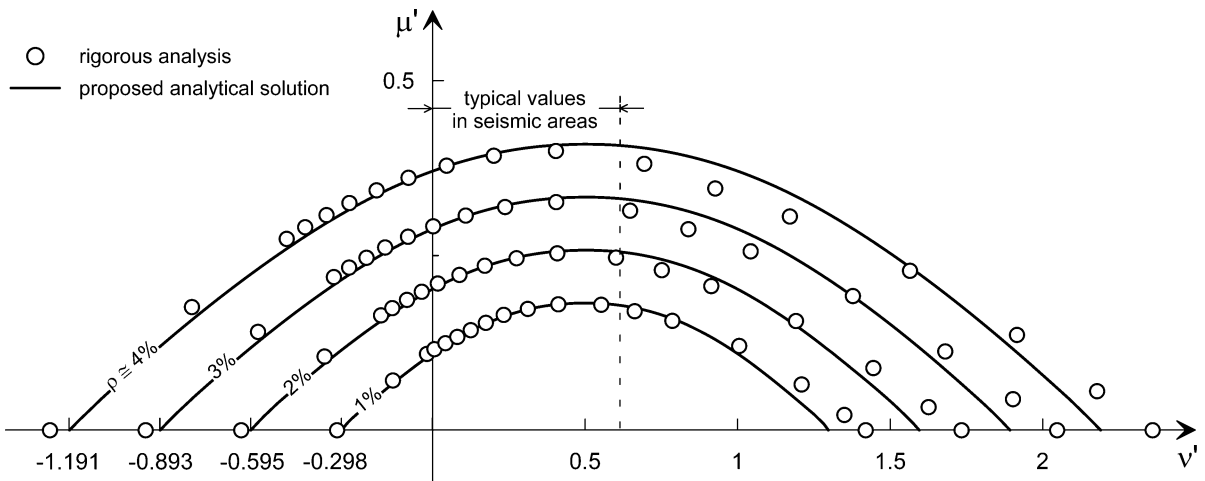


Figure 5

1
2
3

4
5